Department of Pharmaceutics, China Pharmaceutical University, Nanjing, China

Box–Behnken optimization design and enhanced oral bioavailability of thymopentin-loaded poly (butyl cyanoacrylate) nanoparticles

XUEFENG JIN, AIWEN HUANG, QINENG PING, FENG CAO, ZHIGUI SU

Received October 17, 2010, accepted November 3, 2010

Qineng Ping, Department of Pharmaceutics, China Pharmaceutical University, Nanjing 210009, China
pingqn2004@yahoo.com.cn

Pharmazie 66: 339–347 (2011) *doi: 10.1691/ph.2011.0307*

This study was done to prepare thymopentin (TP5)-loaded poly (butyl cyanoacrylate) nanoparticles (TP5-PBCA-NPs) and evaluate thier efficacy for oral delivery. TP5-PBCA-NPs were prepared by emulsion polymerization, and the formulation was optimized based on Box–Behnken experimental design. The physico-chemical characteristics of TP5-PBCA-NPs were evaluated using transmission electron microscopy (TEM), malvern zetasizer, Fourier transform infra-red spectroscopy (FT-IR) and differential scanning calorimetry (DSC). The encapsulation efficiency, enzymatic degradation and release behavior of TP5-PBCA-NPs in various media were evaluated using a high-performance liquid chromatography (HPLC) method. The pharmacodynamic studies on oral administration of TP5-PBCA-NPs were performed in FACScan flow cytometry. An optimum formulation consisted of 0.7% poloxamer 188 (Pol), 0.6% dextran-70 (Dex), 0.1% sodium metabisulfite (Sm), 0.1% TP5 and 1% (v/v) n-butyl cyanoacrylate. The particle size and zeta potential of optimized TP5-PBCA-NPs was 212 nm and −22.6 mV respectively with 82.45% encapsulation efficiency. TP5 was entrapped inside the nanoparticles in molecular dispersion form. The release of TP5 from PBCA-NPs was pH dependent; the cumulative release percentage in 0.1 M HCl for 4 hours was less than 16% while it was more than 80% in pH6.8 PBS. The PBCA-NPs could efficiently protect TP5 from enzymatic degradation; the remained percentage of TP5 encapsulated in PBCA-NPs was 58.40% after incubated with trypsin in pH6.8 PBS for 4 h while it was only 32.29% for free drug. In the oral administration study *in vivo*, the lowered T-lymphocyte subsets values were significantly increased and the raised CD4+/CD8+ ratio was evidently reduced compared with that of TP5 solution ($p < 0.05$), and the improvement of bioavailability was dose-dependent. These results indicated that the PBCA nanoparticles may be a promising carrier for oral delivery of TP5.

1. Introduction

Thymopentin (TP5) is a synthetic pentapeptide (Arg-Lys-Asp-Val-Tyr) corresponding to the 32–36 amino acid sequence of the thymic hormone thymopoietin (TP). It has been shown to have the biologic properties of TP both *in vivo* and *in vitro*, affecting neuromuscular transmission, induction of early T cell differentiation and immune regulation (Goldstein et al. 1979, Goldstein et al. 1985). Clinical studies with TP5 have shown efficacy in the therapy of various diseases including primary and secondary immune deficiencies, autoimmunity, infections and cancers (Singh et al. 1998). However, TP5 is not only severely degraded in the gastrointestinal tract by luminal and membrane-bound enzymes but also rapidly cleaved by plasma proteases in humans (apparent $t_{1/2} = 30$ s) (Heizmann et al. 1996; Tischio et al. 1979). In clinical practice, TP5 is delivered intramuscularly or intravenously. Although such injections benefit from high bioavailability, they fail to provide sustained plasma concentrations and suffer from poor patient compliance due to the required frequency of injections. In order to increase the therapeutic potential, chemical modifications have been tested to obtain stabilized forms of TP5 and multiple drug-carriers have been designed to protect TP5 from enzymatic hydrolysis in the gastrointestinal tract (Chi et al. 2008; Pignatello et al. 2007; Heavner et al. 1986; Zheng et al. 2006; Yin et al. 2006).

Polymer nanoparticles have been extensively investigated to improve oral bioavailability of peptides and protein because nanoencapsulation of peptides and protein colloidal particles protects them against the harsh environment of the gastrointestinal tract, and enhances their transmucosal transport (Des et al. 2006). Various biodegradable polymers like poly-lactic acid (PLA), poly(lactideco-glycolide acid) (PLGA), poly(butyl) cyanoacrylate (PBCA), and chitosan have gained increasing interest as nanocarrier materials. Being different from other polymers, butyl cyanoacrylate has been used in surgical adhesives (Avery and Ord 1982; Leahey et al. 1993). Besides the biocompatibility and biodegradability of PBCA nanoparticles (PBCA-NPs), other inherent advantages, i.e., the simple preparation process and particularly the entrapment of bioactives, specifically proteins and peptides, have made it become the promising drug delivery system (Graf et al. 2009). Human calcitonin and insulin trapped in PBCA nanocapsules showed slower proteolytic degradation than the free peptides in solution, and the plasma pharmacokinetic profiles were consistent with increased survival time of the peptides in the intestine (Lowe and Temple et al. 1994). Dalargin, a Leu-enkephalin analogue (Tyr-*D*Ala-Gly-Phe-Leu-Arg), being loaded in PBCA-NPs, can cross the

Table 1: Box–Behnken experimental design with three independent variables

Batch	Factors			Responses			
	X_1	X_2	X_3	Y_1	Y_2	Y_3	Y_4
1	−1	−1	0	282.9	0.48	−44.7	47.61
2	1	−1	0	176.2	0.07	−35.8	68.94
3	−1	1	0	269.8	0.03	−16.2	85.3
4	1	1	0	171.4	0.11	−12.3	55.2
5	−1	0	−1	210.7	0.08	−2.4	1.38
6	1	0	−1	162.3	0.03	−5.5	0.8
7	−1	0	1	424.5	0.33	−50.7	74.28
8	1	0	1	238.5	0.06	−38.4	62.2
9	0	−1	−1	217.1	0.14	−16.8	2.44
10	0	1	−1	181.5	0.03	−1.6	9.38
11	0	−1	1	354.6	0.32	−61.9	64.24
12	0	1	1	337.8	0.03	−32.3	81.24
13	0	0	0	194.6	0.09	−27.1	72.26
14	0	0	0	213.7	0.06	−19.6	77.97
15	0	0	0	220.7	0.04	−20.3	74.70
16	0	0	0	207.9	0.05	−23.5	73.24
17	0	0	0	189.5	0.12	−19.2	76.51

Table 2: Summary of results of regression analysis for responses Y_1, Y_2, Y_3 and Y_4 for fitting to quadratic model

Quadratic model	R^2	Adjusted R^2	Predicted R^2	SD	% C.V.
Y_1	0.9874	0.9798	0.9692	10.39	4.36
Y_2	0.9788	0.9575	0.9202	0.027	22.05
Y_3	0.9834	0.9735	0.9577	2.76	10.96
Y_4	0.9984	0.9964	0.9957	1.84	3.37

Regression equations of the fitted quadratic model

$Y_1 = 206.55 – 54.94X_1 – 8.79X_2 + 72.98X_3 - 34.40X_1X_3 + 16.93{X_2}^2 + 50.86{X_3}^2$

$Y_2 = 0.075 – 0.083X_1 – 0.10X_2 + 0.057X_3 + 0.12X_1X_2 – 0.057X_1X_3 – 0.044X_2X_3 + 0.047{X_1}^2 + 0.051{X_2}^2$

$Y_3 = –22.97 + 2.75X_1 + 12.10X_2 – 19.63X_3 + 3.85X_1X_3 + 3.60X_2X_3 – 4.73{X_2}^2$

$Y_4 = + 74.94 – 2.68X_1 + 5.99X_2 + 33.49X_3 – 12.86X_1X_2 – 2.88X_1X_3 + 2.51X_2X_3 – 7.67{X_1}^2 – 3.01{X_2}^2 – 32.60{X_3}^2$

[a]Only the terms with statistical significance are included ($p < 0.05$)

blood-brain barrier and induce analgesia after oral application (Schroeder et al. 1998).

In this study, PBCA was selected to design oral nano-carriers for TP5. Because of its highly hydrophilic properties, to incorporate TP5 in hydrophobic nanoparticles is very challenging. In our study, TP5-loaded PBCA-NPs (TP5-PBCA-NPs) with high entrapment efficiency and loading capacity were developed through three-level three-factorial Box–Behnken experimental design. The characteristics of the nanoparticles such as particle size, zeta potential, entrapment efficiency and release behavior were examined. FT-IR and DSC studies assessed the molecular events leading to drug immobilization in the polymer matrix. The effect of protection against enzymatic hydrolysis was investigated in pH 6.8 PBS containing 1% (w/w) trypsin. Using immune dysfunction rats as the pharmacodynamic model, T lymphocyte subsets population as the efficacy index, the immunomodulatory potency of orally administrated TP5-PBCA-NPs was evaluated by FACScan flow cytometry.

2. Investigations, results and discussion

2.1. Formulation optimization of TP5-PBCA-NPs

A three-factor, three-level Box–Behnken statistical experimental design was used to optimize the formulation variables as the response surface methodology requires 17 experiments. Poloxamer 188 and dextran-70, the concentration ranges of which were 0–1.2% and 0–0.8% respectively, were selected as stabilizers in the polymerization process based on previous reports (Douglas et al. 1985). These stabilizers have significant effects on particle size and polydispersion index. Sodium metabisulfite was found to be a very important factor for TP5 loading based on the results from preliminary experimentation, and the concentration for formulation optimization was chosen from 0 to 0.16%.

The independent variables and the responses for all 17 experimental runs are given in Table 1. DEE was found to be significantly higher (47.61–85.30 %) only when the sodium metabisulfite was used at 0.08% or 0.16% concentration level. The ranges of other responses, Y_1, Y_2 and Y_3 were 162.3–424.5 nm, 0.03–0.48 and –61.9–1.6 mv, respectively. All the responses observed for the 17 formulations prepared were simultaneously fitted to first order-, second order- and quadratic models using Design Expert®. The best-fitted model was a quadratic model and the comparative values of R^2, SD and % C.V. are given in Table 2 along with the regression equation generated for each response which was simplified in a stepwise manner ($\alpha_{in} = 0.1$, $\alpha_{out} = 0.1$).

A negative value in regression equation for responses Y_1, Y_2 and Y_3 represents an effect that favors the optimization according to the constraints (Table 3), though a negative value indicates an inverse relationship between the factor and the response. On

Table 3: Variables in Box-Behnken design

Independent variables (Factors)	Level used		
	–1	0	1
X_1 = Poloxamer 188 (% w/v)	0	0.6	1.2
X_2 = Dextran-70 (% w/v)	0	0.4	0.8
X_3 = Sodium metabisulfite (% w/v)	0	0.08	0.16
Dependent variables (Responses)	Constraints		
Y_1 = Particle size (nm)	Minimize and $\leq$ 220 nm		
Y_2 = Polydispersion index (P.I.)	Minimize and $\leq$ 0.1		
Y_3 = Zeta potential (mv)	$\leq$ –20 mv		
Y_4 = Encapsulation efficiency (%)	Maximize and $\geq$ 80%		

the contrary, for Y_4, a positive value represents an effect favoring the optimization. From Table 2, it is evident that X_1 and X_2 have negative effects on the response Y_1 and Y_2 while X_3 has the positive effect on Y_1 and Y_2. These results indicated that as stabilizers, poloxamer 188 and dextran-70 had a high capacity to reduce the particle size and P.I. due to covering on the surface of nanoparticles and avoiding nanoparticles aggregation. Increasing the concentration of sodium metabisulfite would result in larger particle size and higher P.I., which was probably because, in aqueous acidic medium, sodium metabisulfite would exist in the form of $NaHSO_3$ which partly dissociated to produce SO_2. Under high concentration conditions, SO_2 acts as a strong polymerization inhibitor resulting in low molecular weight polymers; however, it was supposed that stabilization by stabilizers was only possible by the agglomeration of the oligomeric subunits in the form of larger nanoparticles (Lescŭre et al. 1992). Then, as a result, nanoparticles with larger size were obtained. For the same reason, increasing stabilizers concentration could lead to the formation of nanoparticles with smaller sizes. On the contrary, response Y_3 has inverse relationship with X_3 while has direct relationship with X_1 and X_2, and the value of Y_3 sharply decreased as increasing X_3 concentration. The decrease of zeta potential may be related to HSO_3^-, and the reason is still unclear. Response Y_4 was also observed to be primarily affected by X_3 which showed direct relationship with Y_4. The reason for this phenomenon could be attributed to absolute zeta potential value increase with the addition of sodium metabisulfite, and the more negative charges probably enhanced the incorporation of TP5 in PBCA-NPs because TP5 molecules with isoelectric point value of 8.59 carried positive charges under acidic conditions (Xin et al. 2007). The effect of X_3 on Y_4 was about 12.5-fold and 5.6-fold as compared to X_1 and X_2, respectively.

Coefficients with higher order terms or more than one factor term in the regression equation represent quadratic relationships or interaction terms, respectively. It also shows that a non-linear relationship exists between responses and factors. Used at different levels in a formulation or when more than one factor are changed simultaneously, a factor can produce a different degree of response. The interaction effect of X_1 and X_3 was favorable for response Y_1 and Y_2, especially for Y_1, whereas it was unfavorable for response Y_3 and Y_4. Highest and positive quadratic effects of X_2 and X_3 were observed for the response Y_1, whereas the negative quadratic effects were seen for the responses Y_4. Higher and positive quadratic effects of X_1 and X_2 were observed for the responses Y_2. Quadratic effect of X_2 was negative for the response Y_3.

Two-dimensional contour plots and three-dimensional response surface plots are presented in Figs. 1–6, which are very useful to study the interaction effects of the factors on the response Y_4. These types of plots are useful to study of the effects of two factors on the response at one time. In all the presented

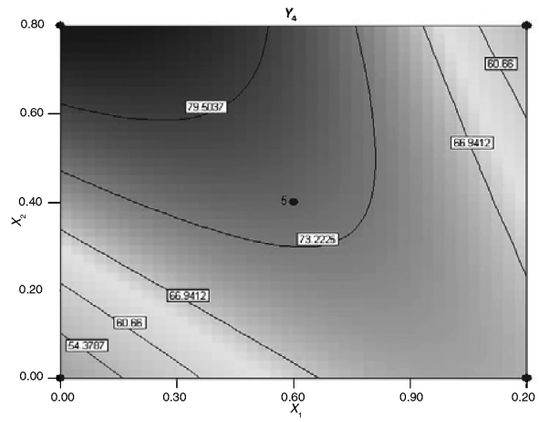

Fig. 1: Contour plot showing effect of poloxamer 188 concentration (X_1) and Dextran-70 concentration (X_2) on encapsulation efficiency (Y_4)

figures, the third factor was kept constant. All the relationships among the three variables are non-linear. Response surface plots show the relationship between these factors even more clearly. Figs. 4 and 6 show that the Y_4 increases with increasing concentration of sodium metabisulfite to about 0.12% at constant concentration of X_1 and X_2. In addition, the interaction effects between X_1, X_2 and X_3 were observed on Y_4 (Fig. 2).

Peyer's patches are the primary induction sites for oral delivery of colloidal particulates, and 200 nm or lower is the optimal particle diameter for particle uptake in Peyer's patches (Jani

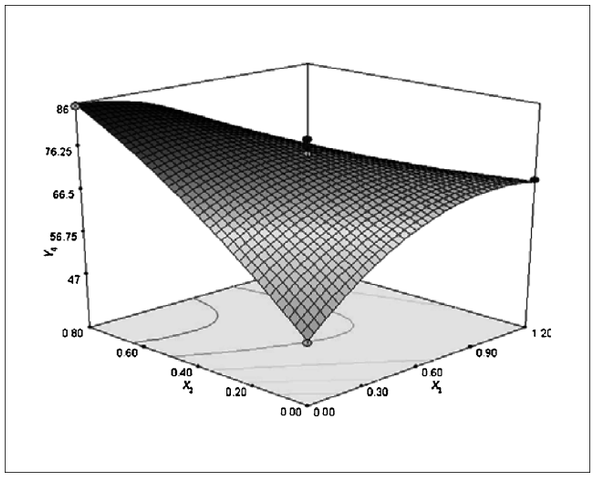

Fig. 2: Response surface plot showing effect of poloxamer 188 concentration (X_1) and Dextran-70 concentration (X_2) on encapsulation efficiency (Y_4)

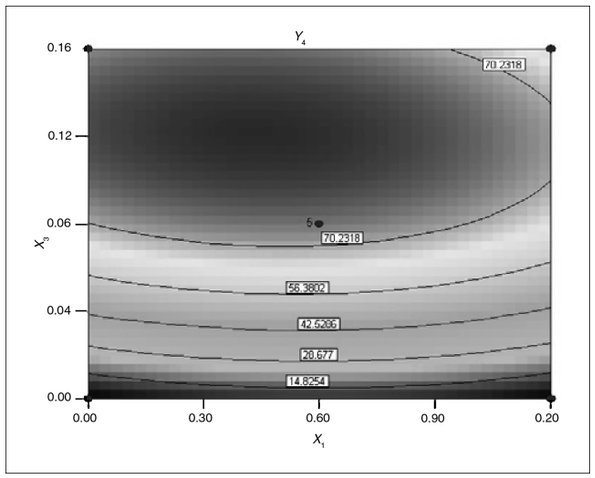

Fig. 3: Contour plot showing effect of poloxamer 188 concentration (X_1) and sodium metabisulfite (X_3) on encapsulation efficiency (Y_4)

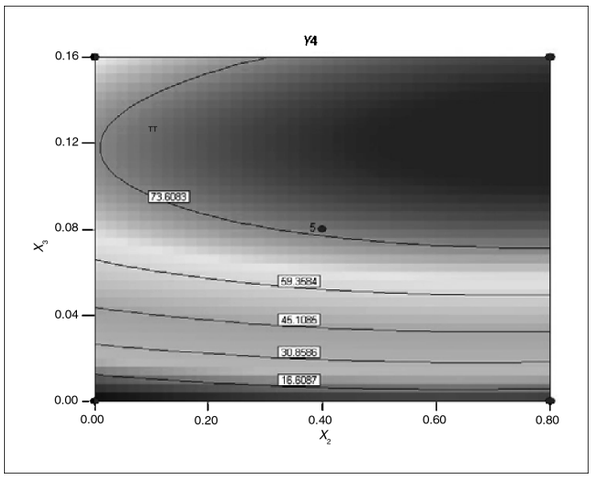

Fig. 5: Contour plot showing effect of Dextran-70 concentration (X_2) and sodium metabisulfite (X_3) on encapsulation efficiency (Y_4)

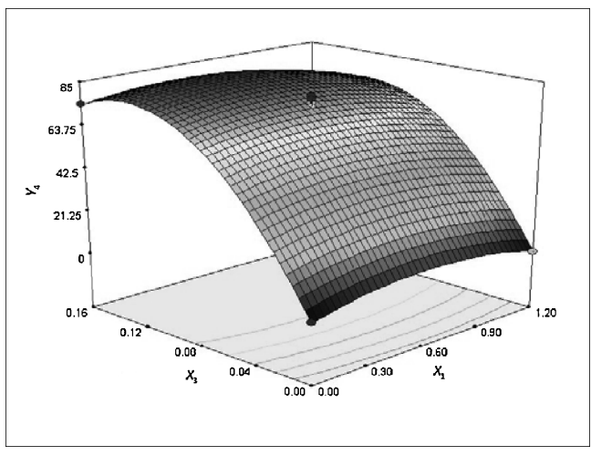

Fig. 4: Response surface plot showing effect of poloxamer 188 concentration (X_1) and sodium metabisulfite (X_3) on encapsulation efficiency (Y_4)

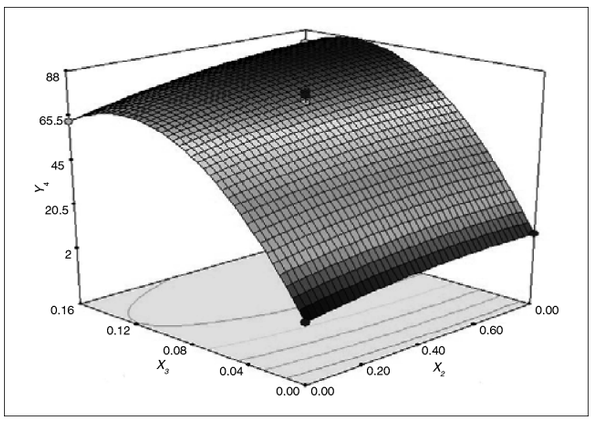

Fig. 6: Response surface plot showing effect of Dextran-70 concentration (X_2) and sodium metabisulfite (X_3) on encapsulation efficiency (Y_4)

et al. 1990; Desai et al. 1996). In our research, most of the particle sizez (11 batches) were not more than 220 nm; hence a, particle size of ≤ 220 nm was selected as the constraint on Y_1. The constraint on Y_2 was minimizing the P.I., moreover, P.I. ≤ 0.1; under this condition, the monodispersed particles with narrow size distribution would be obtained in our study. Previous research reported that PBCA-NPs with zeta potential ≤ -20 mV had good stability (Mulik et al. 2009), and therefore this restriction was applied on Y3. For Y_4, the value of DEE should be attained as big as possible and not less than 80% which could be obtained at present study. The optimum formulation of TP5-PBCA-NPs was selected based on the criteria combining all constraints on Y_1, Y_2, Y_3 and Y_4 (Table 3). Upon 'trading of' various response variables and comprehensive evaluation of feasibility search and exhaustive grid search, the formulation composition with Pol 0.7%, Dex 0.6% and Sm 0.1% was found to fulfill requisites of an optimum formulation. To confirm the validity of the calculated optimal factors and predicted responses, three fresh batches with the optimized formula were prepared and evaluated. As shown in Table 4, the observed response values were very close to the predicted ones.

It is very challenging to incorporate a hydrophilic molecule like TP5 into hydrophobic nanoparticles. The incorporations of TP5 in lipid nanoparticles prepared from O/W or W/O/W microemulsion methods were 5.2% and 1.7%, respectively (Morel et al. 1996). As for lectin-conjugated PLGA nanoparticles, TP5 entrapment efficiency was below 33% (Yin et al. 2006). For multilamellar and plurilamellar liposomes, the encapsulation efficiency were above 75%, but the mass ratio of drug to lipids was about 1.4%(w/w) (Panico et al. 1997). In the present study, TP5 encapsulation efficiency was significantly increased and the drug loading amount was approximately 3.2% (w/w).

Table 4: Composition of checkpoint formulations, the predicted and experimental values of response variables

Optimized formulation composition (X_1:X_2:X_3)	Response variable	Experimental value (mean ± SD, n = 3)	Predicted value
0.7:0.6:0.1	Y1 (nm)	212.3 ± 6.9	217.2
	Y2	0.04 ± 0.015	0.04
	Y3 (mV)	–22.6 ± 0.76	–21.9
	Y4 (%)	82.45 ± 2.31	81.98

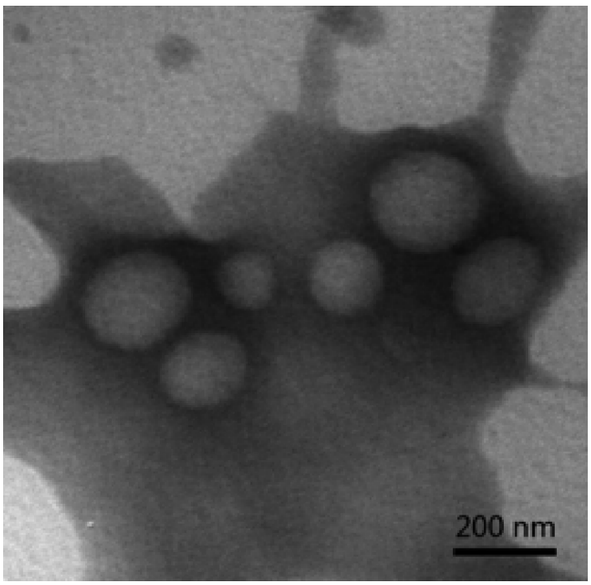

Fig. 7: Transmission electron micrograph of TP5-loaded PBCA nanoparticles (TP5-PBCA-NPs)

2.2. Morphological characterization

The TEM of TP5-PBCA-NPs is shown in Fig. 7. The nanoparticles were spherical in shape with smooth surface. The particle size was observed to be near 200 nm supporting the results of particle size determination by Malvern Mastersizer using dynamic light scattering method.

2.3. FT-IR spectroscopy

FT-IR studies were performed to confirm drug insertion into the nanoparticles. In the FTIR spectrum of TP5 (Fig. 8), the strong bands at $3\,400 \sim 3\,100\,cm^{-1}$ are due to ν_{OH} and ν_{NH}, and the strong band at $1651\,cm^{-1}$ is ascribed to the $\nu_{c\,=\,o}$, $\nu_{C\,=\,N}$, $\delta_{NH3}{}^{+}$, or $\delta_{NH2}{}^{+}$ (Liang et al. 2008). Comparing the FTIR spectrums of TP5-PBCA-NPs (Fig. 9) and PBCA-NPs (Fig. 10), it is evident that all characteristic peaks of PBCA could be found in FTIR spectrum of TP5-PBCA-NPs. The characteristic C ≡ N stretching mode of the polymer was observed at $2250\,cm^{-1}$. The prominent band at $1752\,cm^{-1}$ corresponds to the C = O stretching mode, while the features at 1258 and $1016\,cm^{-1}$ correspond to the asymmetric and symmetric C–O–C stretches, respectively. The CC ≡ N (ν_s) band was observed at $1167\,cm^{-1}$ (Simeonova et al. 2009). However, in FTIR spectrums of TP5-PBCA-NPs the peaks at $3\,400 \sim 3\,100\,cm^{-1}$ and $1642\,cm^{-1}$ were enhanced, which arose from characteristic peaks of TP5 and confirmed the presence of drug molecules in the polymer matrix.

2.4. Differential scanning colorimetry (DSC) of nanoparticles

DSC of n-BCA, PBCA-NPs, TP5-PBCA-NPs and pure TP5 was used to provide additional information on the polymer–drug relationship. The DSC graphs of all the samples are shown in Fig. 11. PBCA thermally degrades via a free radical unzipping reaction with quantitative conversion to monomer (Birkinshaw and Pepper 1986). It has been shown that the nature of the chain end group determines the onset temperature of degradation and therefore DSC should demonstrate if more than one type of chain end or chain type is present (Sullivan et al. 2004). The onset temperature of degradation of PBCA-NPs was 183.0 °C which was very close to that of TP5-PBCA-NPs, 185 °C. This indicates that the same type of chain end groups are present in both, and TP5-PBCA-NPs made of polymer were not initiated by TP5. Compared with graph of n-BCA, it was evident that another peak near 250 °C in graphs of PBCA-NPs and TP5-PBCA-NPs attributed to the endothermic behaviour of n-BCA, which could be supported by previous research (Mulik et al. 2009). As shown in Fig. 9, the thermal behaviour of TP5 was complicated, and the onset temperature of the maximal endothermic peak was found to be 57.0 °C which was in accordance with a previous report (Zheng et al. 2007). As no peak for TP5 was obtained from the graph of TP5-PBCA-NPs, it was clear that TP5 was entrapped inside the nanoparticles in molecular dispersion form; the shift of endothermic peak and difference in ΔH compared to PBCA also suggested the supposition.

2.5. In vitro drug release study

Figure 12 displayed the *in vitro* release profiles of TP5 from TP5-PBCA-NPs at different pH values, and the results showed that release behavior of TP5 was pH dependent. In 0.1 M HCl, a much lower release rate of TP5 from NPs was observed (about 16%) at first 4 h, which was mainly contributed from the free drugs in the nanosuspension. However, at the same time point, the release percentage in pH 5.0 PBS was 40.21%, while in pH 6.8 PBS it was above 80%. The low release rate of TP5 from NPs under acidic conditions was probably due to the following reason: the isoelectric point of TP5 is 8.59, and the amino groups of its molecule will combine with more H^+ at low pH values; then there are strong electrostatic attractions between TP5 and negative charged PBCA-NPs, which results in the release behavior of pH dependent.

The results of *in vitro* drug release study suggested that most of the drug could be entrapped stably in the nanoparticles in stomach environment and then released in intestinal tract for absorption.

2.6. Enzymatic degradation of TP5

The oral peptide administration is mainly precluded by enzymatic degradation of the peptides prior to and during the absorption process. Therefore, it is necessary to evaluate the enzymatic degradation of the TP5-loaded PBCA-NPs. In 0.1 M HCl, there is little TP5 released from TP5-loaded PBCA-NPs, moreover, previous literature reported that degradation of TP5 is not caused by chymotrypsin (Heizmann et al. 1996). For these reasons, the degradation of TP5 was investigated in pH 6.8 PBS containing trypsin. The results of the enzymatic degradation of TP5 in the trypsin are shown in Fig. 13. During the first hours, TP5-loaded PBCA-NPs suspension shows a very similar degradation behavior with TP5 solution because of the free drug not incorporated in nanoparticles, whereas in the following hours the degradation of TP5 in solution is much faster than that loaded in PBCA-NPs. After 4 h, the remained percentage of TP5 free or encapsulated in PBCA-NPs was 32.29% and 58.40%, respectively. It was clear that the degradation of TP5 by trypsin was inhibited due to incorporated in PBCA-NPs. In addition, as supposed, TP5 or TP5-PBCA-NPs incubated with trypsin inactivated by boiling did not show any degradation.

2.7. The effect of oral TP5-PBCA-NPs on immune dysfunction rats

Cyclophosphamide, a known immunosuppressant, was extensively used to establish immune dysfunction models of rats (Doi et al. 1996; Muruganandan et al. 2005; Fen et al. 2007;

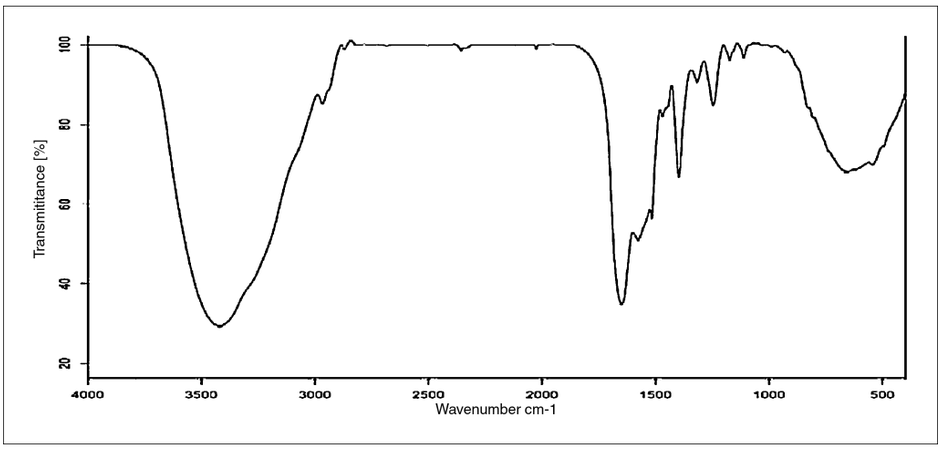

Fig. 8: FTIR spectra recorded in KBr for TP5

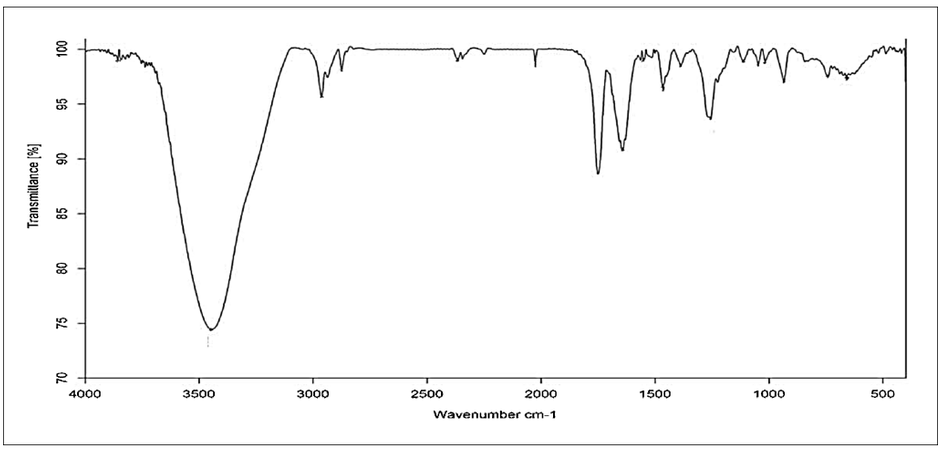

Fig. 9: FTIR spectra recorded in KBr for TP5-PBCA-NPs

Gao et al. 2009). The changes of $CD3^+$, $CD4^+$ and $CD8^+$ T cell population and the $CD4^+/CD^+$ ratios are generally recognized as the index of immune function. After the rats were intraperitoneally primed with cyclophosphamide for 3 days, a series of immune dysfunction symptom was observed (Group 2–6), such as upright hair, reduced appetite, slight diarrhea and diminished activity. As shown in Table 5, the T-lymphocyte percentages of $CD3^+$, $CD4^+$ and $CD8^+$ of the pathological control rats (Group 2) were significantly lowered, and the $CD4^+/CD8^+$ ratio was markedly increased, as compared with those of the normal control rats (Group 1). These results indicated that the T-lymphocyte level of the pathological rats was significantly affected by the immunosuppressant and suggested the pathological model was successfully established.

The level changes of $CD3^+$, $CD4^+$ and $CD8^+$ T-lymphocyte subsets in immune dysfunction rats following administrations

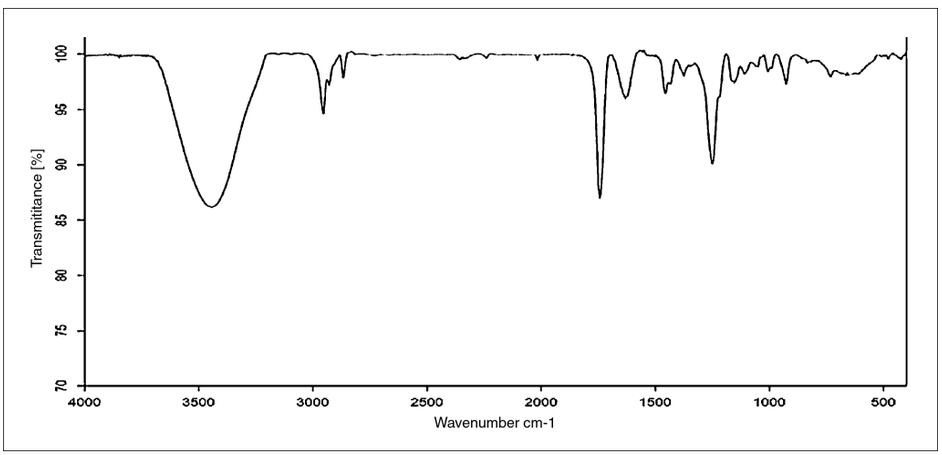

Fig. 10: FTIR spectra recorded in KBr for PBCA-NPs

Table 5: The $CD3^+$, $CD4^+$ and $CD8^+$ lymphocyte subpopulation changes in immunosuppression rats following intravenous injection at a dose of 0.5 mg kg^{-1}·d^{-1} or oral administrations at a dose of 2 mg kg^{-1}·d^{-1} and 4 mg kg^{-1}·d^{-1} TP5 with various formulations for seven consecutive days, respectively.

Groups	Treatment	$CD3^+$ (%)	$CD4^+$ (%)	$CD8^+$ (%)	$CD4^+/CD8^+$
1	Saline	64.74 ± 3.52	42.78 ± 1.94	23.54 ± 1.66	1.82 ± 0.15
2	Saline	31.68 ± 2.45^{a}	23.76 ± 2.43^{a}	7.38 ± 0.70^{a}	3.22 ± 0.22^{a}
3	TP5 solution(2 mg kg^{-1}·d^{-1})	35.84 ± 3.37^{a}	24.32 ± 2.75^{a}	8.52 ± 1.02^{a}	2.87 ± 0.30^{a}
4	TP5-PBCA-NP$_S$(2 mg kg^{-1}·d^{-1})	$48.74 \pm 1.53^{a,b,c}$	$33.76 \pm 1.32^{a,b,c}$	$15.88 \pm 1.58^{a,b,c}$	$2.15 \pm 0.28^{b,c}$
5	TP5-PBCA-NP$_S$(4 mg kg^{-1}·d^{-1})	$56.18 \pm 4.72^{a,b,c}$	$38.48 \pm 3.25^{a,b,c}$	$18.04 \pm 2.07^{a,b,c}$	$2.14 \pm 0.18^{b,c}$
6	TP5, i.v. (0.5 mg kg^{-1}·d^{-1})	$68.06 \pm 2.83^{b,c}$	$45.70 \pm 2.27^{b,c}$	$22.08 \pm 1.40^{b,c}$	$2.08 \pm 0.15^{b,c}$

Group 1 and Group 2 were the normal control and pathological control, respectively. Each value represents the mean ± S.D. (n = 5);
[a] $p < 0.05$ vs. Group 1;
[b] $p < 0.05$ vs Group 2;
[c] $p < 0.05$ vs. Group 3

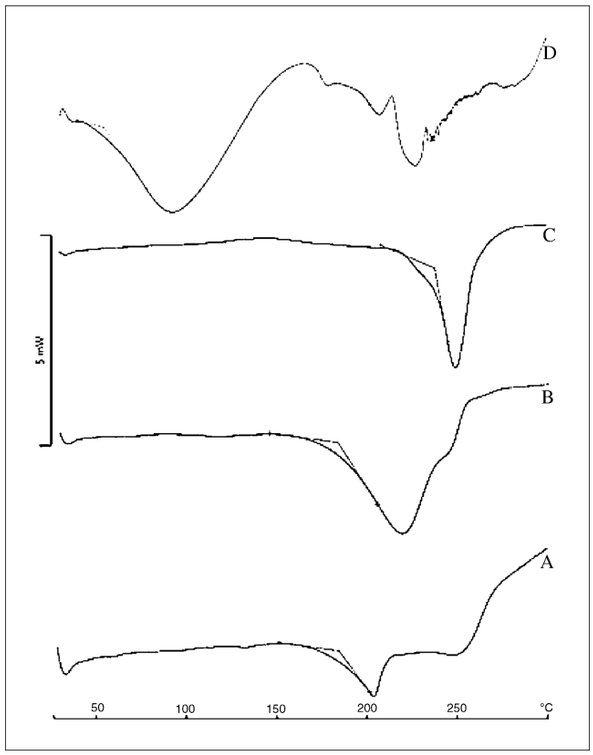

Fig. 11: Differential scanning colorimetry (DSC) study showing characteristic exothermic peaks of TP5-loaded PBCA nanoparticles (A), blank PBCA nanoparticles (B), n-BCA (C), and TP5 (D)

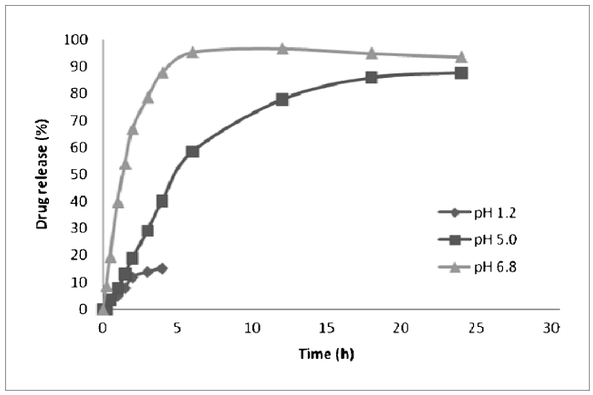

Fig. 12: The cumulative release of TP5 from TP5-PBCA-NPs *in vitro* at different pH value. (mean ± SD, n = 3)

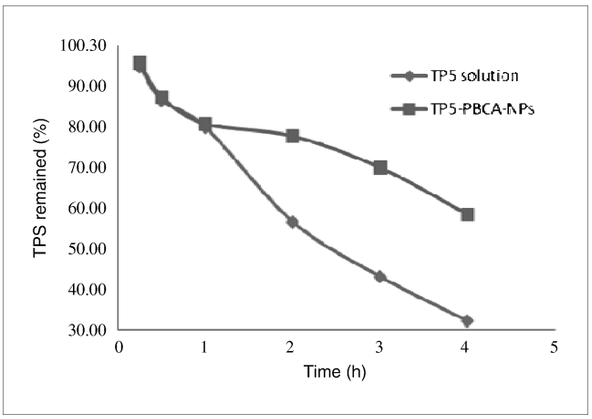

Fig. 13: . Comparing degradation of TP5 from TP5-PBCA-NPs with TP5 solution in PBS (pH 6.8, 0.05 M) containing 1% (w/w) trypsin

with various TP5 formulations and different doses for 7 days (Group 3, 4, 5 and 6) are also shown in Table 5. Compared with those of Group 2, the oral administration of TP5 solution (Group 3) was nearly ineffective, and the $CD3^+$, $CD4^+$ and $CD8^+$ percentages changed little. After intravenous administration of TP5 at a dose of 0.5 mg kg^{-1} once daily for 7 days to the immunosuppression rats (Group 6), all the lowered $CD3^+$, $CD4^+$, and $CD8^+$ values were significantly increased as compared with Group 2, meanwhile, the increased $CD4^+/CD8^+$ ratio was evidently reduced to 2.08; moreover, all the pharmacodynamic indexes were near the normal values ($p > 0.05$). For TP5-PBCA-NPs (Group 4 and Group 5), similar downtrends of the $CD4^+/CD8^+$ ratio and uptrend of $CD3^+$, $CD4^+$ and $CD8^+$ percentages were seen though all the pharmacodynamic indexes were not restored to the normal level ($p < 0.05$). However, to Group 5, due to the increased oral doses, the percentage of T-lymphocyte subsets were higher than Group 4 which means the effect of oral administration TP5-PBCA-NPs was dose-dependent. Interestingly, these results were consistent with the *in vitro* evaluation of biological activity which indicated that TP5-PBCA-NPs could stimulate T cell proliferation (data are not given here).

TP5 is the active sequence of the natural thymopoietin, which enhances the production of thymic T cells and helps to restore immunocompetence. The results indicate that the oral administration of TP5 loaded PBCA nanoparticles is effective for improving the $CD3^+$, $CD4^+$ and $CD8^+$ population and reversing the irregular $CD4^+/CD8^+$ ratio to the normal values. The uptake of nanoparticles by Peyer's patches and protecting incorporated drug from enzymatic hydrolysis may be the major reasons for the improvement of drug bioavailability (Vauthier et al. 2003).

3. Experimental

3.1. Materials

α-Butyl cyanoacrylate monomer was kindly provided by Beijing Suncon Medical Adhesive Co. (China). Poloxamer 188 (Pol) was kindly provided by Beijing Fengli Jingqiu Commerce and Trade Co. (China). Dextran-70 (Dex) was obtained from Shanghai Jingchun Reagent Co. (China). Thymopentin was purchased from Shanghai Soho-Yiming Pharmaceuticals Co. (China). MTT and concanavalin A (Con A) were provided by Sigma (USA). Cyclophosphamide was provided by Jiangsu Hengrui Medicine Co. (China). Fluorescein isothiocyanate (FITC) antirat CD3, Phycoerythrin (PE) antirat CD8a and hemolysin were supplied by eBioscience (USA). Allophycocyanin (APC) antirat CD4 was supplied by Biolegend (USA). All other chemicals were of analytical grade.

3.2. Preparation of TP5-PBCA-NPs

TP5-PBCA-NPs were prepared by emulsion polymerization method (Mulik et al. 2009; Bootz et al. 2004; Behan and Birkinshaw 2001). Briefly, under constant stirring, 50 μl BCA was dropped to 5 ml solution (pH2.0 by HCl) containing required amount of dextran-70, poloxamer 188 and sodium metabisulfite. 20 min later, 5 mg TP5 dissolved in 0.25 ml de-ionized water was introduced. Keeping the polymerization for 4 h under stirring at 800 rpm, the reaction solution was neutralized to pH 4.5 and polymerized for another 1 h. The resulting suspension was filtered to remove agglomerates.

3.3. Experimental design

A three-level three-factorial Box–Behnken experimental design was selected to optimize the formulation factors. This design is suitable for exploring quadratic response surfaces and constructing second-order polynomial models, and is characterized by set of points lying at the midpoint of each edge and center point of the multidimensional cube. The non-linear quadratic model generated by the design is given as

$$Y = b_0 + b_1X_1 + b_2X_2 + b_3X_3 + b_{12}X_1X_2 + b_{23}X_2X_3 + b_{13}X_1X_3 + b_{11}X_1^2 + b_{22}X_2^2 + b_{33}X_3^2$$

where Y represents the response associated with each factor level combination; b_0 is an intercept; b_1 to b_{33} are regression coefficients computed from the observed experimental values of Y (dependent variable); and X_1, X_2 and X_3 are the coded levels of independent variables. In this study, amount of dextran-70, poloxamer 188 and sodium metabisulfite were selected as three independent variables based on the results of preliminary experiments; particle size, zeta potential, polydispersion index and entrapment efficiency (%) with respective constraints were selected as dependent variables (Table 3).

3.4. Nanoparticle characterization

3.4.1. Morphology, Particle size and zeta potential

The morphology of PBCA-NPs was characterized with electronic transmission microscope (TEM) (H-700; Hitachi, Japan) using negative-staining method. The size distribution and zeta potential were determined by Zetasizer (3000HS, Malvern Instruments, UK).

3.4.2. Assay of drug entrapment efficiency (DEE)

Nanoparticle suspension 0.2 ml was diluted with 0.8 ml demineralized water, and was then centrifuged at 15,000 rpm for 30 min. The unloaded drug amount in the supernatant was determined by HPLC (1100 LC, Agilent, USA) at 275 nm through RP C18 column (150 × 6.0 mm, 5 μm, Shimpack, Japan). Mobile phase was consisted of PBS (0.02 mol/L, pH 7.0)-MeOH (87:13, v/v), and the flow rate was 1 ml/min. Instead of demineralized water, tetrahydrofuran was used to mix with the nanoparticles suspension for the assay of total drug amount. DEE was calculated as follows:

$$\text{DEE\%} = (\text{total drug amount} - \text{unloaded drug amount})/\text{total drug amount} \times 100\%$$

3.4.3. Fourier transform infra-red spectroscopy (FT-IR)

FT-IR spectra of the nanoparticles (with and without drug) or TP5 were recorded in KBr pellets on a Perkin Elmer 1000 FTIR spectrometer with resolution of 2 cm^{-1}. A total of 64 scans were used and data were recorded over the range 4000–400 cm^{-1}.

3.4.4. Differential scanning colorimetry (DSC) of nanoparticles

Thermal analysis of n-BCA, PBCA-NPs, TP5-PBCA-NPs and pure TP5 was used to provide additional information on the polymer–drug relationship and the nature of formed nanoparticles. An automatic thermal analyzer system (DSC 204, Netzsch, Germany) was used for characterization with a 5 mg sample in hermetically sealed aluminium pans heated from 25 °C to 300 °C at a constant rate of 10 °C/min. Inert atmosphere was maintained by nitrogen purging at a flow rate of 20 ml/min (Mulik et al. 2009).
PBCA-NPs were prepared according to method 3.2 but without TP5 and Sm.

3.4.5. In vitro drug release studies

In vitro release studies of TP5 from PBCA-NPs were performed as follows. Nanoparticle suspension 2 ml or the drug solution containing 2.0 mg/ml of TP5 was transferred into a dialysis bag. The dialysis bags were then dipped into 100 ml of 0.1 M HCl (pH 1.2), phosphate buffer solution (0.2 M, pH 5.0), and phosphate buffer solution (0.05 M, pH 6.8), respectively. All the solutions were incubated in water-bath shaker at 37 °C with constant orbital mixing (60 rpm). At specified time intervals, 1 ml of release medium were withdrawn for HPLC assay and 1 ml fresh media was added. The cumulative release of TP5 from the nanoparticles was calculated. All the operations were performed in triplicate.

3.5. Enzymatic degradation of TP5

Trypsin 1:250 (100 mg, of > 1000 N.F.U/mG, EC 3.4.21.4, Amresco) was suspended in 10 ml prewarmed (37 °C) PBS (0.05 M, pH 6.8). After a 30-min activation period, TP5 was added into the solution at the final concentration of 0.06 mM with the formulation of free or encapsulated in PBCA-NPs. At specified time intervals after TP5 added, 200 μl aliquots were taken from the incubated solution and diluted with an equal volume of ice-cold 1 M perchloric acid to stop enzymatic degradation. TP5 concentrations in aliquots were determined as discribed in *3.4.2*. Blanks were obtained by incubating the TP5 or TP5-PBCA-NPs with trypsin 1:250 inactivated by boiling. The degradation rate was indicated by remained percentage of TP5.

3.6. In vivo pharmacodynamic studies

3.6.1. Immunosuppression model rats

All animal experiments complied with the requirements of the National Act on the use of experimental animals (China). 30 normal female Sprague–Dawley rats (180–210 g, the experimental animal center of Zhejiang province) were equally divided into six groups (five each) and fasted but had free access to water for 12 h before the experiments. Group 1 as a normal control was per orally given physiological saline once daily for 10 days. Group 2 through Group 6 were intraperitoneally primed with cyclophosphamide in a dose of 35 mg $kg^{-1}\cdot d^{-1}$ at the first 3 days for construction of immunosuppression model (Li et al. 1996; Sŭn. et al. 2000). From the fourth day, once daily for 7 days, Group 2 as an immunosuppression control were given with physiological saline orally, and Group 3 through Group 5 received the following TP5 formulations: (1) TP5 solution, 2 mg $kg^{-1}\cdot d^{-1}$; (2)TP5-PBCA-NPs, 2 mg $kg^{-1}\cdot d^{-1}$; (3) TP5-PBCA-NPs, 4 mg $kg^{-1}\cdot d^{-1}$. The sixth group was primed with TP5 solution at a dose of 0.5 mg $kg^{-1}\cdot d^{-1}$ intravenously. 200 μl blood of each rat was collected at the eleventh day via the caudal vein placed into heparinized tubes, and stored at 4 °C until flow cytometry analysis.

3.6.2. Flow cytometry analysis

Lymphocyte populations were determined by multiparameter flow cytometry with three-color analyses as follows (Yin et al. 2006; Wang et al. 2006). Anticoagulant blood 100 μl, 2 μl CD3-FITC, 5 μl CD4-APC and 5 μl CD8a-PE were added to test tube, mixed by vortex for 30 s and incubated at room temperature and darkness for 20 min. Then 2 ml hemolysin was added and incubated for another 10 min. After the red cells were lysed completely, the specimens were centrifuged at 2000 rpm for 5 min. The sediment cells were collected, washed with 2 ml physiological saline twice, fixed in 0.5 ml of 1% paraformaldehyde, and then the $CD3^+$, $CD4^+$ and $CD8^+$ T-lymphocyte subsets were measured within 4 h using FACSCalibur flow cytometer with CELLQuest software (Becton Dickinson, USA) for acquisition and analysis. The values of $CD3^+$ T cell counts, $CD4^+$ T cell counts and $CD8^+$ T cell counts, as well as the ratios of $CD4^+$ and $CD8^+$ were calculated for the evaluation of immunocompetence.

3.6.3. Statistical analysis

Mean values and standard deviations (SD) of recorded parameters were calculated. For comparison between the experimental groups and corresponding controls, the analysis of variance ANOVA followed by post hoc

Student-Newman-Keuls test (SPSS 13; SPSS Int., Chicago, IL, USA) was applied. A value of $p < 0.05$ was considered to be significant.

Acknowledgement: This research work was granted by the national science and technology of China for new drugs development with a major project number of 2009ZX09310-004.

References

Avery BS, Ord RA (1982) The use of butyl cyanoacrylate as a tissue adhesive in maxillo-facial and cranio-facial surgery. Br J Oral Surg 20: 84–95.

Behan N, Birkinshaw C (2001) Preparation of poly(butyl cyanoacrylate) nanoparticles by aqueous dispersion polymerisation in the presence of insulin. Macromol Rapid Comm 22: 41–43.

Birkinshaw C, Pepper DC (1986). The thermal degradation of polymers of n-butylcyanoacrylate prepared using tertiary phosphine and amine initiators. Polym Degrad Stab, 16:241–59.

Bootz A, Vogel V, Schubert D, Kreuter J (2004) Comparison of scanning electron microscopy, dynamic light scattering and analytical ultracentrifugation for the sizing of poly(butyl cyanoacrylate) nanoparticles. Eur J Pharm Biopharm 57: 369–375.

Chi Q, Xie X, Zhang J, Yang Y, Li Z, Mei X (2008) Synthesis, characterization and biological activities of thymopentin ethyl ester. Pharmazie, 63 (11): 784–787.

Des Rieux A, Fievez V, Garinot M, Schneider YJ, Preat V (2006) Nanoparticles as potential oral delivery systems of proteins and vaccines: a mechanistic approach. J Control Release 116: 1–27.

Desai MP, Labhasetwar V, Amidon GL, Levy RJ (1996) Gastrointestinal uptake of biodegradable microparticles: effect of particle size. Pharm Res 13 (12): 1838–1845.

Doi T, Nagai H, Tsukuda R, Suzuki T (1996) Dose-response relationships of cytotoxicity, PFC response and histology in the spleen in rats treated with alkylating agents. Toxicology 107: 47–60.

Douglas SJ, Ilium L, Davis SS (1985) Particle size and size distribution of poly(butyl 2-cyanoacrylate) nanoparticles. II: Influence of stabilizers. J Colloid Interface Sci 103: 154–163.

Fen Xia Hou HFY, Tao Yu, Wei Chen, (2007) The immunosuppressive effects of 10 mg/kg cyclophosphamide in Wistar rats. Environ Toxicol Pharmacol 24: 30–36.

Gao J, Ding X, Chu C, Lu L, Zhang Y, Chen Y, Fan W, Li G, Gao S (2009) Dry powder inhalations containing thymopentin and its immunomodulating effects in Wistar rats. Eur J Pharm Sci 36: 572–579.

Goldstein G, Audhya TK (1985) Thymopoietin to thymopentin: experimental studies. Surv Immunol Res 4 Suppl 1: 1–10.

Goldstein G, Scheid MP, Boyse EA, Schlesinger DH, Van Wauwe J, (1979) A synthetic pentapeptide with biological activity characteristic of the thymic hormone thymopoietin. Science 204: 1309–1310.

Graf A, MacDowell A, Rades T (2009) Poly(alkylcyanoacrylate) nanoparticles for enhanced delivery of therapeutics - is there real potential? Expert Opin Drug Deliv 6: 371–387.

Heavner GA, Kroon DJ, Audhya T, Goldstein G (1986) Biologically active analogs of thymopentin with enhanced enzymatic stability. Peptides 7: 1015–1019.

Heizmann J, Langguth P, Biber A, Oschmann R, Merkle HP, Wolffram S (1996) Enzymatic cleavage of thymopoietin oligopeptides by pancreatic and intestinal brush-border enzymes. Peptides 17:1083–1089.

Jani P, Halbert GW, Langridge J, Florence AT (1990) Nanoparticle uptake by the rat gastrointestinal mucosa: quantitation and particle size dependency. J Pharm Pharmacol 42: 821–826.

Leahey AB, Gottsch JD, Stark WJ (1993) Clinical experience with N-butyl cyanoacrylate (Nexacryl) tissue adhesive. Ophthalmology 100: 173–180.

Lescure F, Zimmer Z, Roy D, Couvreur P (1992) Optimization of polyalkylcyanoacrylate nanoparticle preparation: Influence of sulfur dioxide and pH on nanoparticle characteristics. J Colloid Interface Sci 154: 77–86.

Li LQ, Wang JX, Song DM, Fan SG, Mei L (1996) Building up of an animal model of conditioned immunosuppression and analysis of its possible mechanism. Yao Xue Xue Bao 31: 477–480.

Liang Yong-tao XZ-b, Wang Ming-zhe, Zhao Shuang, Wang En-si (2008). Spectral Data Analysis and Identifi cation of Thymopentin. Chin J Pharm 39: 120–122.

Lowe PJ, Temple CS (1994) Calcitonin and insulin in isobutylcyanoacrylate nanocapsules: protection against proteases and effect on intestinal absorption in rats. J Pharm Pharmacol 46: 547–552.

Morel S, Ugazio E, Cavalli R, Gasco MR (1996) Thymopentin in solid lipid nanoparticles. Int J Pharm 132: 259–261.

Mulik R, Mahadik K, Paradkar A (2009) Development of curcuminoids loaded poly(butyl) cyanoacrylate nanoparticles: Physicochemical characterization and stability study. Eur J Pharm Sci 37: 395–404.

Muruganandan S, Lal J, Gupta PK (2005) Immunotherapeutic effects of mangiferin mediated by the inhibition of oxidative stress to activated lymphocytes, neutrophils and macrophages. Toxicology 215: 57–68.

Panico A, Pignatello R, Cardile V, Puglisi G (1997) Preparation of liposome formulations containing immunomodulatory peptides. Pharm Acta Helv 72: 1–10.

Pignatello R, Pecora TM (2007) Conjugation of thymopentin (TP5) with lipoamino acid residues increases the hydrolytic stability and preserves the biological activity. Pharmazie 62: 663–667.

Schroeder U, Sommerfeld P, Sabel BA (1998) Efficacy of oral dalargin-loaded nanoparticle delivery across the blood-brain barrier. Peptides 19: 777–780.

Simeonova M, Ivanova G, Enchev V, Markova N, Kamburov M, Petkov C, Devery A, O'Connor R, Brougham D (2009) Physicochemical characterization and *in vitro* behavior of daunorubicin-loaded poly(butylcyanoacrylate) nanoparticles. Acta Biomater 5: 2109–2121.

Singh VK, Biswas S, Mathur KB, Haq W, Garg SK, Agarwal SS (1998) Thymopentin and splenopentin as immunomodulators. Current status. Immunol Res 17: 345–368.

Sullivan CO, Birkinshaw C (2004) *in vitro* degradation of insulin-loaded poly (n-butylcyanoacrylate) nanoparticles. Biomaterials 25: 4375–4382.

Sun DL PZS, Wang YF, Chen HP, Wu HG, Zhai DD (2000) Effect of medicinal vesiculation on hematopoeisis function of rats treated by cyclophosphamide chemotherapy. Zhe Jiang Zhong Yi Xue Yuan Xue Bao 24:74–78.

Tischio JP, Patrick JE, Weintraub HS, Chasin M, Goldstein G (1979) Short *in vitro* half-life of thymopoietin 32–36 pentapeptide in human plasma. Int J Pept Protein Res 14: 479–484.

Vauthier C, Dubernet C, Fattal E, Pinto-Alphandary H, Couvreur P (2003) Poly(alkylcyanoacrylates) as biodegradable materials for biomedical applications. Adv Drug Deliv Rev 55: 519–548.

Wang J, Lu WL, Liang GW, Wu KC, Zhang CG, Zhang X, Wang JC, Zhang H, Wang XQ, Zhang W (2006) Pharmacokinetics, toxicity of nasal cilia and immunomodulating effects in Sprague-Dawley rats following intranasal delivery of thymopentin with or without absorption enhancers. Peptides 27: 826–835.

Xin Li LZ, Yonghui Chang, Shubao Shen, Hanjie Ying, Pingkai Ouyang (2007) Kinetics of adsorption of thymopentin on a gel-type strong cation-exchange resin. Chromatogr Sci Ser 66: 231–235.

Yin Y, Chen D, Qiao M, Lu Z, Hu H (2006) Preparation and evaluation of lectin-conjugated PLGA nanoparticles for oral delivery of thymopentin. J Control Release 116: 337–345.

Zheng Ai-ping LM-g, Wang Jian-cheng, Zhang Qiang., (2007) Study on preparation release *in vitro* and biological activity of thymopentin-loaded pH-sensitive chitosan nanoparticles for oral administration. Chin Pharm J 42: 679–685.

Zheng AP, Wang JC, Lu WL, Zhang X, Zhang H, Wang XQ, Zhang Q (2006) Thymopentin-loaded pH-sensitive chitosan nanoparticles for oral administration: preparation, characterization, and pharmacodynamics. J Nanosci Nanotechnol 6: 2936–2944.